

Neutral strange particle production at mid unit rapidity in $p + p$ collisions at $\sqrt{s} = 200$ GeV

J. Adams¹ and M. Heinz² for the STAR collaboration

¹University of Birmingham, UK

²University of Bern, Switzerland

December 2, 2024

Abstract

We briefly discuss the methods of analysing reconstructed neutral strange particles in $p + p$ collision data measured at $\sqrt{s} = 200$ GeV taken using the Solenoidal Tracker At RHIC (STAR) detector. We present spectra for K_S^0 , Λ and $\bar{\Lambda}$ as a function of p_T and multiplicity, and compare to previous high energy $p + \bar{p}$ collision data. The two component nature of the spectra suggests contributions from hard and soft processes, and the observed increase of $\langle p_t \rangle$ with multiplicity indicates a growing contribution from the hard processes. The work described herein was presented as a poster at the Quark Matter 2004 conference.

1 Introduction

Particles which contain strange quarks are valuable probes of the dynamics of $p + p$ collisions, as constituent strange quarks are not present in the initial colliding nuclei. The relative enhancement of the strange particle yield per participant nucleon from $p + p$ collisions to heavy ion collisions has been suggested as a possible Quark Gluon Plasma signature [1]. The strangeness yield in $p + p$ collisions is particularly important because it forms the baseline from which any possible strangeness enhancement in Au+Au collisions is determined. We report the first measurements of inclusive neutral strange particle production in $p + p$ collisions at a centre of mass energy (\sqrt{s}) of 200 GeV. The data was acquired during the 2001-2002 run and approximately 10 million events were available for analysis. We compare the Λ , $\bar{\Lambda}$ and K_S^0 spectra with previous $p + \bar{p}$ collision data taken at \sqrt{s} between 200 and 1800 GeV.

2 Analysis

The STAR experiment consists of a number of detectors and is described in detail elsewhere [2],[3]. Neutral strange particle decays, v0s, were identified by analysing the tracks made by their charged daughter particles. The following decay channels were used in order to reconstruct Λ , $\bar{\Lambda}$ and K_S^0 candidates:

$$\Lambda \rightarrow p + \pi^- \text{ (69\%)} \quad \bar{\Lambda} \rightarrow \bar{p} + \pi^+ \text{ (69\%)} \quad K_S^0 \rightarrow \pi^+ + \pi^- \text{ (64\%)}$$

Daughter particle identification was achieved by analysing the specific ionisation energy loss ($\frac{dE}{dx}$) of tracks. Combinatorial background mainly formed by the random crossings of oppositely charged tracks was reduced by the application of topological cuts (e.g a distance of closest approach of the v0 candidates daughter tracks). In the analysis corrections were made for the primary vertex finding and v0 finding efficiencies by embedding Monte Carlo tracks into real data. Using a previous measurement of the Ξ^- yield it was possible to make an estimate of the feed down correction for Λ and $\bar{\Lambda}$.

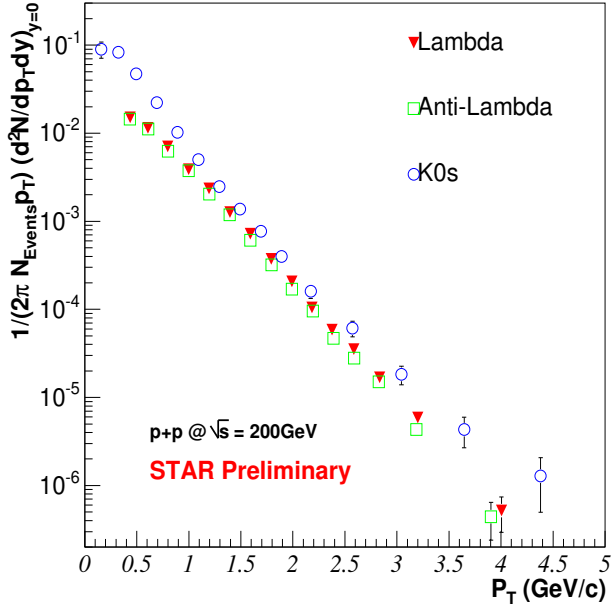


Figure 1: Minimum-bias, non-feed down corrected, Λ , $\bar{\Lambda}$, and K_S^0 spectra with ($|y| \leq 0.5$) from $p + p$ at $\sqrt{s} = 200\text{GeV}$. The errors in the plot are statistical only.

3 Study of yield and $\langle p_T \rangle$

Non-feed down corrected, minimum bias trigger, spectra for Λ , $\bar{\Lambda}$ and K_S^0 , are superposed in Figure 1. As the fiducial region of the TPC limits the p_T acceptance at mid-rapidity to greater than 0.3 GeV (Λ) and greater than 0.1 GeV (K_S^0), it is necessary to fit the data and extrapolate the fit function in order to determine total particle yields and $\langle p_T \rangle$.

Previous $p + \bar{p}$ experiments UA5[4] and UA1[5] used exponentials in m_T and p_T , and power law functions to fit the strange spectra. With this higher statistics measurement we have found that none of these functions alone is able to describe the data well over the whole p_T range. A better parameterisation is obtained with a two component fit. An exponential function in m_T provides a good description of the data at $p_T \leq 1$ GeV, whereas at high p_T an exponential in p_T ($\Lambda, \bar{\Lambda}$) or a power law (K_S^0) describes the data. Therefore composite fits, represented in equations 1 (for $\Lambda, \bar{\Lambda}$) and 2 (for K_S^0), were applied to the data shown in Figure 1. The $\langle p_T \rangle$ and dN/dy were extracted by integrating the fits over all p_T and are tabulated in table 1. A full study of the systematic errors is in progress but we estimate an uncertainty in the range of 10%. The errors quoted in table 1 are the variations in dN/dy and $\langle p_T \rangle$ when individual exponentials in m_T and p_T and power laws are fitted to the spectra.

$$\frac{1}{2\pi p_T} \frac{d^2N}{dy dp_T} = A.e^{-\frac{m_T}{T}} + B.e^{-\frac{p_T}{T}} \quad (1)$$

$$\frac{1}{2\pi p_T} \frac{d^2N}{dy dp_T} = C.e^{-\frac{m_T}{T}} + D.(1 + \frac{p_T}{p_0})^{-n} \quad (2)$$

Particle	dN/dy	dN/dy in measured p_T region \pm stat	dN/dy feed down corrected	$\langle p_T \rangle$
Λ	0.044 ± 0.003	0.038 ± 0.001	0.034 ± 0.005	0.76 ± 0.05
$\bar{\Lambda}$	0.042 ± 0.003	0.036 ± 0.001	0.032 ± 0.005	0.75 ± 0.05
K_S^0	0.123 ± 0.006	0.115 ± 0.001		0.60 ± 0.05

Table 1: A summary of dN/dy and $\langle p_T \rangle$ for neutral strange particles in $p + p$ at $\sqrt{s} = 200$ GeV with $|y| \leq 0.5$. The errors quoted are statistical + systematic, where the systematic error is estimated from the results of different fits to the data

The UA5 experiment [4] measured Λ , $\bar{\Lambda}$ and K_S^0 in $p + \bar{p}$ collisions at $\sqrt{s} = 200$ GeV. In order to compare dN/dy over the STAR rapidity range ($|y| \leq 0.5$), the UA5 ($|y| \leq 2.0$) yield has been scaled according to the STAR rapidity interval,

Particle	STAR dN/dy $ y \leq 0.5$	UA5 dN/dy $ y \leq 2.0$	UA5 dN/dy $ y \leq 0.5$
$\Lambda + \bar{\Lambda}$	0.066 ± 0.004	0.27 ± 0.07	0.08 ± 0.02
$\frac{\Lambda + \bar{\Lambda}}{2K_S^0}$	0.27 ± 0.04	0.31 ± 0.09	0.31 ± 0.09

Table 2: A summary of dN/dy for $\Lambda + \bar{\Lambda}$ and $\frac{\Lambda + \bar{\Lambda}}{2K_S^0}$ ($\Lambda, \bar{\Lambda}$ feed down corrected) measured by the UA5 [4] and STAR experiments at $\sqrt{s} = 200$ GeV

Particle	STAR $\langle p_T \rangle$ $ y \leq 0.5$	UA5 $\langle p_T \rangle$ $ y \leq 2.0$
$\Lambda + \bar{\Lambda}$	0.76 ± 0.05	$0.8 +0.2,-0.14$
K_S^0	0.60 ± 0.05	$0.53 +0.08,-0.06$

Table 3: A summary of $\langle p_T \rangle$ for $\Lambda + \bar{\Lambda}$ (feed down corrected) and K_S^0 measured by the UA5 [4] and STAR experiments at $\sqrt{s} = 200$ GeV

using the rapidity distribution for $\Lambda, \bar{\Lambda}$ and K_S^0 generated from a Pythia simulation [6]. A comparison of the dN/dy is tabulated in table 2 and a comparison of $\langle p_T \rangle$ in table 3. The dN/dy and $\langle p_T \rangle$ measured by STAR and UA5 agree within the quoted errors. This indicates that at mid-rapidity and $\sqrt{s} = 200$ GeV, particle production does not depend greatly on the net baryon number of the colliding nuclei.

4 $\langle p_T \rangle$ vs Multiplicity

Figure 2 shows that the $\langle p_T \rangle$ of the Λ and K_S^0 increases with measured (uncorrected) track multiplicity. This result is similar to the trend observed by UA1 [5] and E735 [7] and is consistent with the idea of the $\langle p_T \rangle$ and multiplicity increasing with the momentum transfer of the parton-parton collisions. The correlation between $\langle p_T \rangle$ and multiplicity may be due to increasing strange particle production from harder processes such as jet and mini-jet fragmentation mechanisms [8].

In Figure 3 we confine the spectra into six multiplicity classes and divide by the minimum-bias spectrum. From Figures 1 and 3 we can infer that for all event multiplicity classes the low p_T part of the spectra dominates the yield, indicating that soft particle production occurs readily for all types of events which can be characterised by event multiplicity. The correlation between $\langle p_T \rangle$ and multiplicity shown in Figure 2 is driven by the low p_T ($p_T < 1.5$ GeV) particles as panels a) and b) in Figure 3 show an increase in the low p_T region as multiplicity increases. For low multiplicity classes there is a large deficit of high p_T particles and for high multiplicity classes, where there is more momentum transfer, there is a large enhancement.

Panel c in Figure 3 shows the Λ to K_S^0 ratio for high, minimum-bias and low multiplicity classes. It indicates that at high p_T , Λ production is relatively more favoured over K_S^0 for high multiplicity events, and that K_S^0 production is relatively favourable for low multiplicity events. This is perhaps because the Λ , being more massive than the K_S^0 , is harder to produce in low multiplicity collisions, where there is less momentum transfer.

5 Conclusions and future work

The STAR experiment has made the first high statistics measurements of mid-rapidity $\Lambda, \bar{\Lambda}$, and K_S^0 generated in $p + p$ collisions at $\sqrt{s} = 200$ GeV. The measured $\langle p_T \rangle$ and dN/dy agree with those measured by the UA5 collaboration for $p + \bar{p}$ at $\sqrt{s} = 200$ GeV. We have shown that the $\bar{\Lambda}$ yield is very similar to the Λ yield which indicates that there is small net baryon number at mid-rapidity. We observe an increase in the $\langle p_T \rangle$ with measured multiplicity for Λ and K_S^0 , which indicates a growing contribution from harder processes. Furthermore the multiplicity integrated spectra are best described by a two component fit. This implies that the particle production mechanism is one which produces significant quantities of soft strange hadrons, best described by an exponential in m_T as well as higher p_T strange hadrons, which are best described by power law or p_T exponential functions. A study of the systematic errors and a more thorough feed down correction for Λ and $\bar{\Lambda}$ is underway.

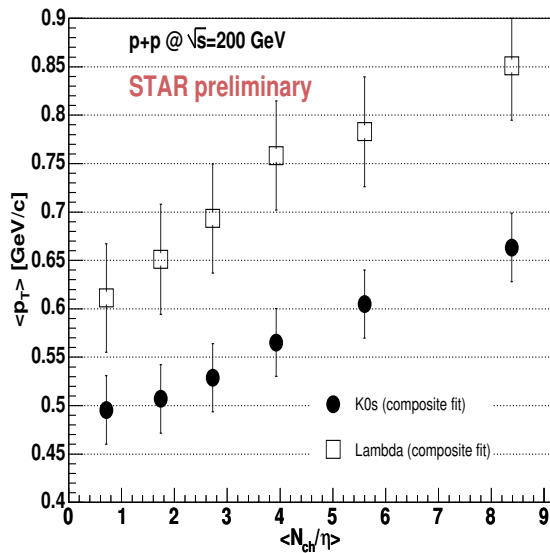


Figure 2: $\langle p_T \rangle$ vs charged uncorrected multiplicity per unit pseudo rapidity, (uncorr N_{ch}/η) obtained with composite function fits. A hardening of the spectra is observed with increasing event multiplicity. The errors in the plot are statistical only.

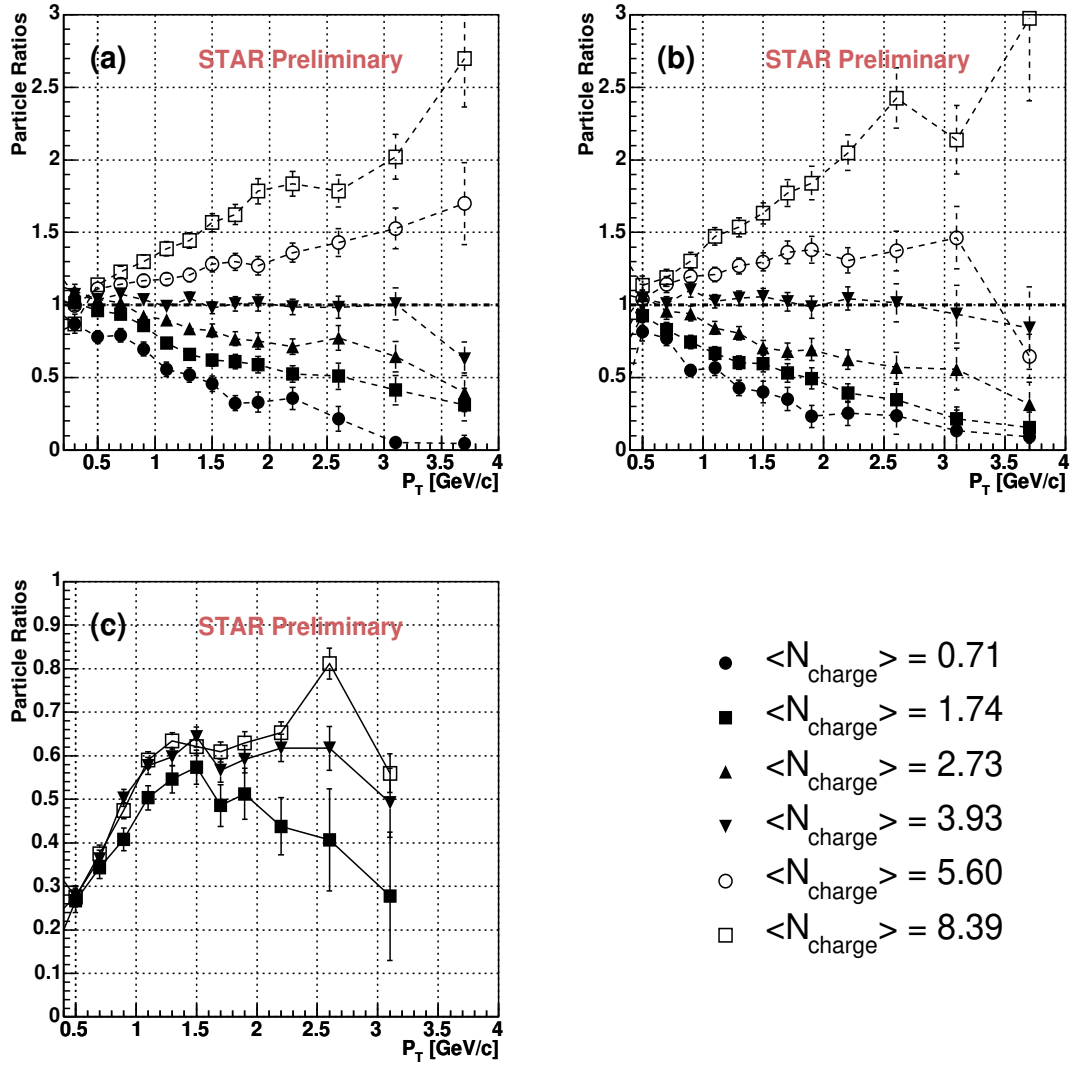


Figure 3: Spectra for K_S^0 (a) and Λ (b) normalised by the min-bias distribution for different uncorrected multiplicity classes. Panel c shows the ratio of Λ / K_S^0 in the lowest (filled squares) and highest multiplicity bin (open squares) as well as the ratio of the min bias result (filled triangles). The errors are statistical

References

- [1] J.Rafelski and B. Muller, Phys. Rev. Lett. 48, 1066 (1982)
- [2] K.H.Ackermann et al, (STAR Collaboration), Nucl. Phys. A661, 681c (1999)
- [3] K.H.Ackermann et al, (STAR Collaboration), NIM
- [4] R.E.Ansgore et al, (UA5 Collaboration) Nucl. Phys. B328, 36 (1989)
- [5] G. Bocquet et al (UA1 Collaboration), Phys. Lett. B 366, 441 (1996)
- [6] T. Sjostrand et al. Pythia 6.2, Physics and Manual, hep/01208264 (2002)
- [7] T.Alexopolous et al (E735), Phys. Rev. D Vol 48 , 3, 984 (1993)
- [8] X. Wang, M. Gyulassy, Phys. Lett. B 282, 466 (1992)